



## Electrical behaviour of MIS devices based on Si nanoclusters embedded in SiO<sub>x</sub>Ny and SiO<sub>2</sub> films

Emmanuel Jacques, Laurent Pichon, Olivier Debieu, Fabrice Gourbilleau

### ► To cite this version:

Emmanuel Jacques, Laurent Pichon, Olivier Debieu, Fabrice Gourbilleau. Electrical behaviour of MIS devices based on Si nanoclusters embedded in SiO<sub>x</sub>Ny and SiO<sub>2</sub> films. *Nanoscale Research Letters*, 2011, 6, pp.170. 10.1186/1556-276X-6-170 . hal-00618107

**HAL Id: hal-00618107**

**<https://hal.science/hal-00618107>**

Submitted on 31 Aug 2011

**HAL** is a multi-disciplinary open access archive for the deposit and dissemination of scientific research documents, whether they are published or not. The documents may come from teaching and research institutions in France or abroad, or from public or private research centers.

L'archive ouverte pluridisciplinaire **HAL**, est destinée au dépôt et à la diffusion de documents scientifiques de niveau recherche, publiés ou non, émanant des établissements d'enseignement et de recherche français ou étrangers, des laboratoires publics ou privés.

**NANO EXPRESS**

**Open Access**

# Electrical behavior of MIS devices based on Si nanoclusters embedded in $\text{SiO}_x\text{N}_y$ and $\text{SiO}_2$ films

Emmanuel Jacques<sup>1\*</sup>, Laurent Pichon<sup>1</sup>, Olivier Debieu<sup>2</sup>, Fabrice Gourbilleau<sup>2</sup>

## Abstract

We examined and compared the electrical properties of silica ( $\text{SiO}_2$ ) and silicon oxynitride ( $\text{SiO}_x\text{N}_y$ ) layers embedding silicon nanoclusters (Sinc) integrated in metal-insulator-semiconductor (MIS) devices. The technique used for the deposition of such layers is the reactive magnetron sputtering of a pure  $\text{SiO}_2$  target under a mixture of hydrogen/argon plasma in which nitrogen is incorporated in the case of  $\text{SiO}_x\text{N}_y$  layer. Al/ $\text{SiO}_x\text{N}_y$ -Sinc/p-Si and Al/ $\text{SiO}_2$ -Sinc/p-Si devices were fabricated and electrically characterized. Results showed a high rectification ratio ( $>10^4$ ) for the  $\text{SiO}_x\text{N}_y$ -based device and a resistive behavior when nitrogen was not incorporating ( $\text{SiO}_2$ -based device). For rectifier devices, the ideality factor depends on the  $\text{SiO}_x\text{N}_y$  layer thickness. The conduction mechanisms of both MIS diode structures were studied by analyzing thermal and bias dependences of the carriers transport in relation with the nitrogen content.

## Introduction

Silicon heterojunctions have been extensively studied for the understanding of the physics of the device as well as their applications to majority of the carrier rectifier [1], photodetectors [2], solar cells [3], and indirect gap injection lasers [4]. Because of its indirect band gap, silicon is a highly inefficient material for a light emitter. However, to overcome this problem, different approaches were developed in this last decade for the fabrication of Si-based light emitting sources made of silicon nanoclusters (Sinc) embedded in silica or silicon oxynitride ( $\text{SiO}_2$ -Sinc or  $\text{SiO}_x\text{N}_y$ -Sinc) matrix.

Due to quantum confinement effects, Sinc are characterized by an energy band gap which is enlarged with respect to bulk silicon and by an intense room temperature photoluminescence that can be obtained in the visible-near infrared (IR) range [5,6]. Previous study [7] recently reported that the presence of incorporated nitrogen species influences the silicon nanoclusters' growth and affects the photoluminescence of the  $\text{SiO}_x\text{N}_y$ -Sinc layer. In addition, IR light emitting properties were also reported in matrix embedding Sinc and rare earth [8-11]. In such system, the emitting rare earth ions benefit from the quantum

confinement properties of the carriers generated within Sinc to be efficiently excited by an energy transfer mechanism. Electroluminescence of  $\text{SiO}_x\text{N}_y$ -Sinc-based IR light emitting devices is limited by the difficulty in carrier injection. Therefore, prior to developing IR light emitting devices, a good understanding of optimum carrier injection in  $\text{SiO}_x\text{N}_y$ -Sinc type layers is needed. In this way, previous works have been recently reported on electrical properties in metal-insulator-semiconductor (MIS) devices fabricated with such silicon-rich oxide layers either deposited by (1) plasma-enhanced chemical vapor deposition technique [12] or by (2) magnetron co-sputtering of Si,  $\text{SiO}_2$  [13]. In the first case, rectifying behavior was observed, but not in the second. In addition, thermal dependence of the carrier transport was not studied.

In this present work, we report a detailed study of the carrier transport governing electrical properties of  $\text{SiO}_2$ -Sinc and  $\text{SiO}_x\text{N}_y$ -Sinc layers integrated in MIS devices. Layers are deposited by reactive magnetron sputtering of a pure  $\text{SiO}_2$  cathode. The thermal and the bias dependences of the carrier transport are analyzed. The aim of such study consists in fabricating a thin layer for future electroluminescent devices doped with rare earth ions. Thus, one of the key parameters is to overcome the insulating characteristic of the  $\text{SiO}_2$  matrix by incorporating nitrogen.

\* Correspondence: emmanuel.jacques@univ-rennes1.fr

<sup>1</sup>Groupe Microélectronique, IETR, UMR CNRS 6164, Campus de Beaulieu, Rennes Cedex, 35042 France

Full list of author information is available at the end of the article

### Device technology and experimental details

Devices are elaborated on p-type (111)-oriented silicon substrates with resistivity in the range 0.001-0.005  $\Omega$  cm (see inset of the Figure 1a). A  $\text{SiO}_2$ -Sinc (or  $\text{SiO}_x\text{N}_y$ -Sinc) layer was deposited by reactive magnetron sputtering of a pure  $\text{SiO}_2$  target under a mixture of hydrogen/argon plasma. In the case of  $\text{SiO}_x\text{N}_y$  layer, nitrogen gas

is incorporated in the plasma leading to a final concentration of 15 at.% in the film. For more details on the deposition process, see ref. [14]. Two thicknesses  $d$  of 30 and 65 nm were deposited for each layer, which was subsequently submitted to an optimized annealing treatment at 1,050°C during 30 min under  $\text{N}_2$  flux. Next, aluminum was thermally evaporated on active layer.

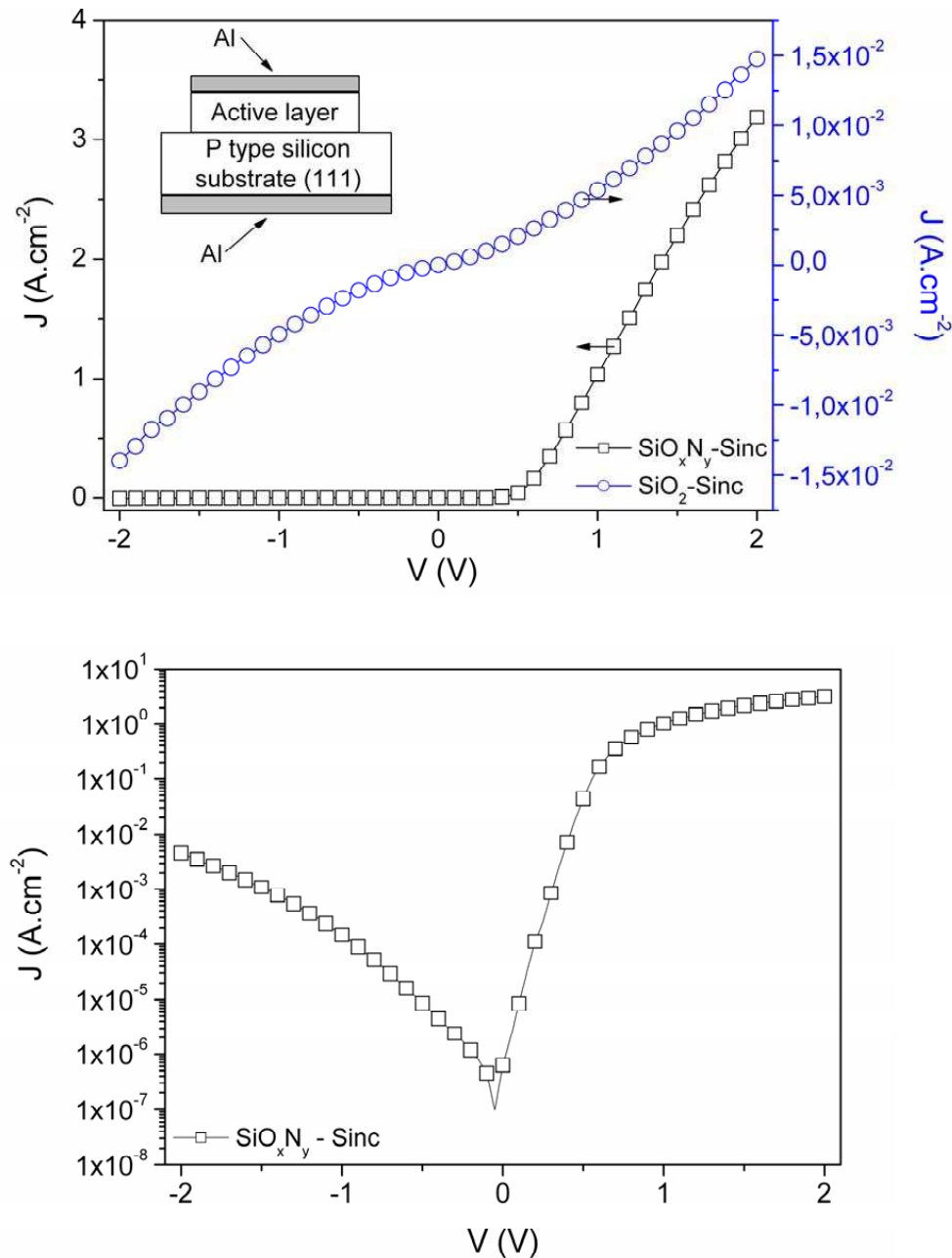


**Figure 1 Comparison of devices.** (a) Linear current density-voltage characteristics of MIS structure based on  $\text{SiO}_2$ -Sinc and  $\text{SiO}_x\text{N}_y$ -Sinc layer. Inset: Schematic cross section of the tested MIS structures, (b) current density-voltage characteristics of MIS structure based on  $\text{SiO}_x\text{N}_y$ -Sinc layer plotted in semi log scale.

Both aluminum and active layers were patterned by wet etching to define the geometry of the device. A second thermal evaporation of aluminum on the back surface was carried out to ensure the ohmic contact with the p-type crystalline silicon. Finally, the devices were annealed into forming gas ( $H_2$  to  $N_2$ , 10%) at  $390^\circ\text{C}$  during an optimum duration of 30 min to stabilize the electrical properties of the devices.

Static electrical characteristics  $J(V)$  are collected by using an HP 4155B semiconductor parameter analyzer. For temperature measurements from  $-70^\circ\text{C}$  to  $230^\circ\text{C}$  samples are placed in a cryostat under vacuum ( $10^{-5}$ - $10^{-4}$  Pa). All measurements were made in darkness on more than 20 devices homogeneously located over the 2-in. surface substrate. The area of each tested device is  $0.32\text{ mm}^2$ .

## Results

The comparison of the devices'  $J(V)$  characteristics of  $\text{SiO}_x\text{N}_y$ -Sinc and  $\text{SiO}_2$ -Sinc-based devices reveals a high rectifying behavior for the former while no rectifying behavior is observed for the latter (Figure 1a).  $J(V)$  electrical characteristics for  $\text{SiO}_2$ -Sinc layer is typical of conduction in (semi) insulating material. Such a result suggests that the rectifying behavior of the  $\text{SiO}_x\text{N}_y$ -Sinc layer could be explained by the presence of the incorporated nitrogen acting as N-type doping specie [15]. In this case, at low forward bias ( $0\text{ V} \leq V \leq 0.8\text{ V}$ ), current density taking account serial resistance can be described by:

$$J = J_0 \left( \exp \frac{qV - RJ}{nk_B T} - 1 \right) \quad (1)$$

where  $q$  is the electron charge,  $k_B$  the Boltzmann's constant,  $n$  the ideality factor dealing with current dominated by carrier diffusions ( $n = 1$ ) and/or by carriers recombination processes at defects ( $n = 2$ ),  $R$  the global serial resistance and  $J_0$  the saturation current density. Ideality factor  $n$  and serial resistance  $R$  are deduced by fitting our experimental results with the theoretical model (1). The resistance  $R$  is likely to arise from minority carrier space charge, the bulk resistances, and finally contact resistance. In our case,  $n$  was estimated to  $n \approx 1.2$  indicating that carrier injection is dominated by the carrier diffusion process. For such N-rich devices  $J(V)$  plots have an excellent rectifying ratio ( $> 10^4$  at  $V = \pm 1\text{ V}$ ) (Figure 1b) leading to a higher injected current level than reported in the literature [16-18]. In addition, at high voltages ( $2\text{ V} > V > 0.8\text{ V}$ ), current deviates from the exponential behavior due to the low global resistance series ( $20\ \Omega < R < 40\ \Omega$ ).

Studies of bias and temperature dependence of the electrical properties are carried out to analyze the

carrier transports for the two devices. Several models are currently used to understand the carrier injection. For  $\text{SiO}_x\text{N}_y$ -Sinc-based devices biased in the reverse mode, the Poole-Frenkel (PF) model is the most convenient. In this approach, electrons are considered to be thermally emitted from the randomly distributed traps to the conduction band as a result of the lowering of the columbic potential barrier by an external electric field. This model is described by the following relation [19]:

$$J = N\mu E \exp \left( -\frac{\phi_0}{k_B T} \right) \exp \left( \frac{\beta_{PF} E^{1/2}}{k_B T} \right) \quad (2)$$

where  $J$  is the current density,  $N$  the density of trapping sites,  $\mu$  the effective carrier mobility,  $E (= V/d)$  the local electric field,  $\phi_0$  the zero field trapped energy barrier depth and  $\beta_{PF}$  the PF coefficient.

This latter is extracted from the linear representation of  $\ln(J/E) = f(E^{1/2})$  (Figure 2) and is related to the permittivity of active layer, and thus to the material composition, following the relation:

$$\beta_{PF} = \left( \frac{q^3}{\pi \epsilon_0 \epsilon_r} \right)^{1/2} \quad (3)$$

The permittivity obtained is also compared to the value deduced from quasi static C-V measurements. The coefficients deduced from the PF relation provides  $\epsilon_r = 5.6$  and  $\epsilon_r = 4.4$  for the 30-nm and the 65-nm-thick  $\text{SiO}_x\text{N}_y$ -Sinc layers, respectively while from C-V measurements, the corresponding permittivity obtained are  $\epsilon_r = 5.1$  and  $\epsilon_r = 4.3$ . Such similar results are consistent with values obtained with the PF model to explain the

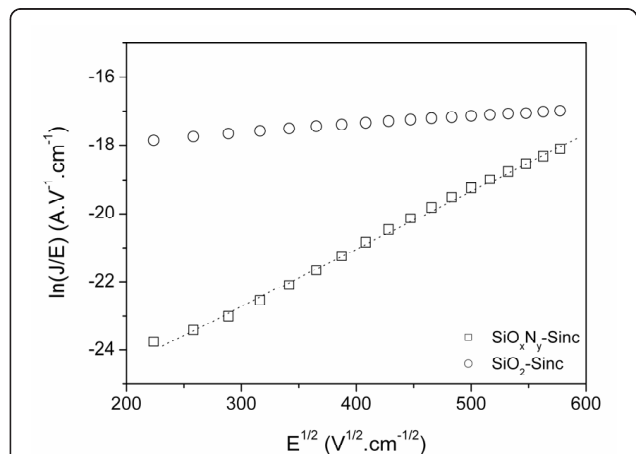


**Figure 2** Plots of the  $\ln(J/E)$  vs  $E^{1/2}$  of  $\text{Al}/\text{SiO}_x\text{N}_y$ -Sinc/p-Si and  $\text{Al}/\text{SiO}_2$ -Sinc/p-Si structures.

reverse current behavior ( $V < -0.2$  V). The difference of permittivity noticed could be explained either by a change of the density of Si nanoclusters (for the same Si content) or by a modification of the Si excess with the thickness. Considering that we observe an increase of the refractive index from 1.61 to 1.75 for 65 nm and the 30-nm layer thicknesses respectively, it suggests that during the first step of the deposition process, the starting growth process conditions could promote the incorporation of Si within a few nanometres thick due to the vicinity of the Si substrate.

Temperature measurements of the reverse current have been carried out in order to confirm the Poole-Frenkel mechanism for which the current is thermally activated. Thus, the corresponding activation energy  $E_a$  is defined by the following relation:

$$E_a = \varphi_0 - \beta_{PF} E^{1/2} \quad (4)$$

Arrhenius diagrams of  $\ln(J)$  vs  $1/T$  (Figure 3) show a temperature dependence of the reverse current that confirms a thermal activation of the current and consequently that the carrier transport follows a PF mechanism. The carriers' emission from defects following such a mechanism is enhanced by a barrier lowering where the electrical field is the most important, that means at the PN junction interface. In this way, the Poole-Frenkel emission of carriers may likely occur from defects in the bulk of the  $\text{SiO}_x\text{N}_y$  matrix located at Sinc/ $\text{SiO}_x\text{N}_y$  interfaces [12] close to the p-type silicon substrate.

For low temperatures,  $J$  does not depend on the temperature indicating that it is more representative of a tunnel conduction way. This behavior is more pronounced at high reverse bias because of the linear decrease of the  $J/E^2 = f(1/E)$  plot (Figure 4) according to the Fowler-Nordheim model given as [20]:

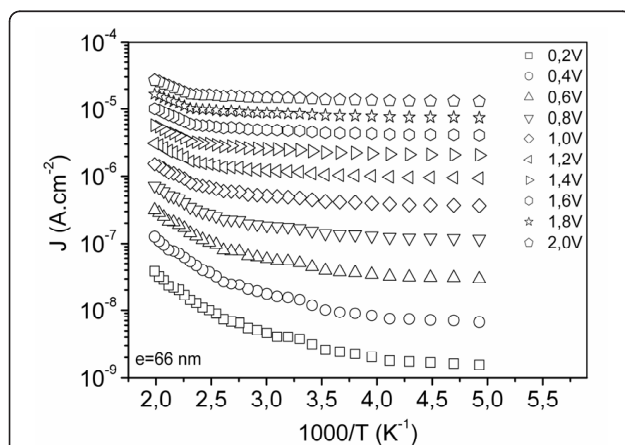


**Figure 3** Arrhenius representations of the current density of the  $\text{SiO}_x\text{N}_y$ -Sinc layer made MIS structures.

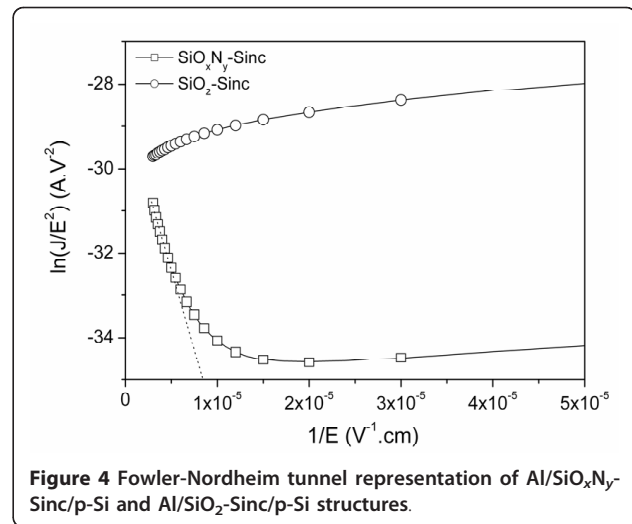


**Figure 4** Fowler-Nordheim tunnel representation of  $\text{Al}/\text{SiO}_x\text{N}_y$ -Sinc/p-Si and  $\text{Al}/\text{SiO}_2$ -Sinc/p-Si structures.

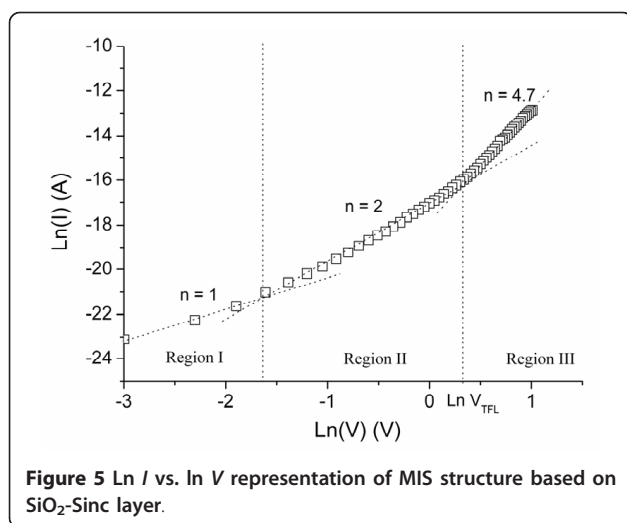
$$J = CE^2 \exp \left( - \frac{4\sqrt{2m^*} (\Phi_B)^{3/2}}{3qhE} \right) \quad (5)$$

where  $C$  is a constant both depending on the elementary charge  $q$ , the barrier height  $\Phi_B$ , and the Planck's constant  $h$ , and where  $m^*$  stands for the carriers' effective mass. This conduction mechanism could be effective between the silicon nanoclusters through the silicon oxynitride.

The same approach has been used for the N-free Si-rich layer. No current variation in the  $\text{SiO}_2$ -Sinc layer according to the electric field has been observed (Figure 2) demonstrating that Poole-Frenkel mechanism is not the conduction mode in such an MIS structure. Fowler-Nordheim tunneling conduction has also been tested for this layer (see Figure 4) and no variation is observed following equation 5. Therefore, the electrical behavior of this layer in both reverse and forward bias cannot be explained by Fowler-Nordheim tunneling conduction. However, the forward current characteristics plotted with a representation in  $\ln(I) = \ln(V)$  in Figure 5 can be divided into three regions. In this case, the current follows a voltage power law ( $I \propto V^n$ ). In the first region ( $V < 0.2$  V)  $n = 1$  corresponding to an ohmic behavior where the deduced intrinsic resistivity of the material ( $\rho = 2.7 \times 10^{11} \Omega \text{ cm}^{-1}$ ) is typical of (semi) insulator. For higher voltages ( $0.2 \text{ V} < V < 0.4 \text{ V}$ ), conduction mechanism is due to space charge limited conduction dominated by a discrete trapping level in the second region ( $n = 2$ ) and by exponential distribution in the third region ( $n > 2$ ). From this characteristic, the density  $n_t$  of the trapped electrons can be extracted accordingly:

$$n_t = \frac{2\varepsilon\varepsilon_0}{qd^2} V_{TFL} \quad (6)$$





where  $\varepsilon$  is the permittivity of the material and  $V_{TFL}$  is the voltage at which the current significantly increases. The permittivity extracted from C-V measurements is  $\varepsilon_r = 3.95$ .  $V_{TFL}$  is defined as the intersection between the linear parts of the second and the third region. The value of the trap density  $n_t$ , acting as quality factor of the SiO<sub>2</sub>-Sinc layer, has been estimated to be  $5.39 \times 10^{16} \text{ cm}^{-3}$ . The presence of trap centers could be associated to the density of Si nanoclusters in the silicon oxide matrix as it has been reported in a previous work [21]. In the case of SiO<sub>x</sub>N<sub>y</sub> layer, as previously discussed, conduction mechanism appears to be different. In such a layer, the nitrogen is suspected to passivate the trap centers close to the silicon nanoclusters and thus promoting N-type doping effect responsible of pn junction creation between the active layer and the P-doped silicon substrate.

## Conclusion

Conduction mechanisms of SiO<sub>2</sub>-Sinc and SiO<sub>x</sub>N<sub>y</sub>-Sinc layers have been studied and compared. The use of silicon oxynitride with embedded silicon nanoclusters has been validated in order to achieve diode with high rectifying behavior. Nitrogen significantly modifies the electrical behavior of the layer. It is suspected to be both responsible of a of (1) a defect passivation at the interface of silicon oxide matrix and silicon nanoclusters and (2) to act as N-doping specie and to promote a pn junction creation between active layer and P-doped silicon substrate.

This study has shown the interest to use nitrogen in silicon matrix with silicon nanoclusters to improve the current injection in the MIS structure. This effect could be interesting for an energy transfer to the rare earth ions for an infrared emission in such structures based on silicon-rich oxynitride layer doped with rare earth.

## Acknowledgements

This work was financially supported by the *Agence National de la Recherche* (France) through the program PNANO-ANR-08-NANO-005 entitled DAPHNES (*Dispositifs Appliqués à la Photonique à base de Néodyme et de Silicium*).

## Author details

<sup>1</sup>Groupe Microélectronique, IETR, UMR CNRS 6164, Campus de Beaulieu, Rennes Cedex, 35042 France <sup>2</sup>Centre de Recherche sur les Ions, les Matériaux et la Photonique, UMR CEA/CNRS/ENSICAEN/UCBN 6 boulevard du Maréchal Juin, Caen Cedex 4, 14050 France

## Authors' contributions

EJ fabricated and electrically characterized the devices, he also analysed the conduction mechanisms of the devices and wrote a part of the manuscript. LP analysed and explained the conduction mechanisms in the device and participated in the writing of the manuscript. OD fabricated the thin films and carried out the optical and microstructural characterizations. FG conceived of the study and participated in the coordination of the project. All authors read and approved the final manuscript.

## Competing interests

The authors declare that they have no competing interests.

Received: 20 September 2010 Accepted: 24 February 2011

Published: 24 February 2011

## References

- Matsuura H, Okuno T, Okushi H, Tanaka K: Electrical properties of n-amorphous/p-crystalline silicon heterojunctions. *J Appl Phys* 1984, **55**:1012.
- Zhang TC, Guo Y, Mei ZX, Gu CZ, Du XL: Visible-blind ultraviolet photodetector based on double heterojunction of n-ZnO/insulator-MgO/p-Si. *Appl Phys Lett* 2009, **94**:113508.
- Xu Y, Hu Z, Diao H, Cai Y, Zhang S, Zeng X, Hao H, Liao X, Fortunato E, Martins R: Heterojunction solar cells with n-type nanocrystalline silicon emitters on p-type c-Si wafers. *J Non-Cryst Solids* 2006, **352**:1972.
- Marinace JC: Tunnel Diodes by Vapor Growth of Ge on Ge and on GaAs. *IBM J Res Dev* 1960, **4**:280.
- Min KS, Shcheglov KV, Yang CM, Atwater HA, Brongersma ML, Polman A: Defect-related versus excitonic visible light emission from ion beam synthesized Si nanocrystals in SiO<sub>2</sub>. *Appl Phys Lett* 1996, **69**:2033.
- Priolo F, Franzo G, Pacifici D, Vinciguerra V, Iacona F, Irrera A: Role of the energy transfer in the optical properties of undoped and Er-doped interacting Si nanocrystals. *J Appl Phys* 2001, **89**:264.
- Bolduc M, Genard G, Yedji M, Barba D, Martin F, Terwagne G, Ross GG: Influence of nitrogen on the growth and luminescence of silicon nanocrystals embedded in silica. *J Appl Phys* 2009, **105**:013108.
- Iacona F, Pacifici D, Irrera A, Miritello M, Franzo G, Priolo F, Sanfilippo D, Di Stefano G, Fallica PG: Electroluminescence at 1.54  $\mu\text{m}$  in Er-doped Si nanocluster-based devices. *Appl Phys Lett* 2002, **81**:3242.
- Gourbilleau F, Levallois M, Dufour C, Vicens J, Rizk R: Optimized conditions for an enhanced coupling rate between Er ions and Si nanoclusters for an improved 1.54- $\mu\text{m}$  emission. *J Appl Phys* 2004, **95**:3717.
- Seo SY, Kim MJ, Shin J: The Nd-nanocluster coupling strength and its effect in excitation/de-excitation of Nd<sup>3+</sup> luminescence in Nd-doped silicon-rich silicon oxide. *Appl Phys Lett* 2003, **83**:2778.
- Gourbilleau F, Belarouci A, Breard D, Dufour C, Rizk R: Active emitters based on nanostructured Si. *Int J Nanotechnol* 2008, **5**:574.
- Prezioso S, Anopchenko A, Gaburro Z, Pavesi L, Pucker G, Vanzetti L, Bellutti P: Electrical conduction and electroluminescence in nanocrystalline silicon-based light emitting devices. *J Appl Phys* 2008, **104**:063103.
- Jambois O, Berencen Y, Hijazi K, Wojdak M, Kenyon AJ, Gourbilleau F, Rizk R, Garrido B: Current transport and electroluminescence mechanisms in thin SiO<sub>2</sub> films containing Si nanocluster-sensitized erbium ions. *J Appl Phys* 2009, **106**:063526.
- Ternon C, Gourbilleau F, Portier X, Voidevel P, Dufour C: An original approach for the fabrication of Si/SiO<sub>2</sub> multilayers using reactive magnetron sputtering. *Thin Solid Films* 2002, **419**:5.

15. Temple-Boyer P, Jalabert L, Couderc E, Scheid E, Fadel P, Rousset B: **Properties of nitrogen doped silicon films deposited by LPCVD from disilane and ammonia.** *Thin Solid Films* 2002, **414**:13.
16. Pellegrino P, Garrido B, Arbiol J, García C, Lebour Y, Morante JR: **Site of Er ions in silica layers codoped with Si nanoclusters and Er.** *Appl Phys Lett* 2006, **88**:121915.
17. Anopchenko A, Marconi A, Moser E, Prezioso S, Wang M, Pavesi L, Pucker G, Bellutti P: **Low-voltage onset of electroluminescence in nanocrystalline-Si/SiO<sub>2</sub> multilayers.** *J Appl Phys* 2009, **106**:033104.
18. Wong JI, Chen TP, Yang M, Liu Y, Ng CY, Ding L: **Current conduction in Al/Si nanocrystal embedded SiO<sub>2</sub>/p-Si diodes with various distributions of Si nanocrystals in the oxide.** *J Appl Phys* 2009, **106**:013718.
19. Harrell WR, Frey J: **Observation of Poole-Frenkel effect saturation in SiO<sub>2</sub> and other insulating films.** *Thin Solid Films* 1999, **352**:195.
20. Lenzlinger M, Snow EH: **Fowler-Nordheim Tunneling into Thermally Grown SiO<sub>2</sub>.** *J Appl Phys* 1969, **40**:278.
21. Rafiq MA, Tsuchiya Y, Mizuta H, Oda S, Uno S, Durrani ZAK, Milne W: **Charge injection and trapping in silicon nanocrystals.** *Appl Phys Lett* 2005, **87**:182101.

doi:10.1186/1556-276X-6-170

**Cite this article as:** Jacques *et al.*: Electrical behavior of MIS devices based on Si nanoclusters embedded in SiO<sub>x</sub>N<sub>y</sub> and SiO<sub>2</sub> films. *Nanoscale Research Letters* 2011 **6**:170.

**Submit your manuscript to a SpringerOpen<sup>®</sup> journal and benefit from:**

- Convenient online submission
- Rigorous peer review
- Immediate publication on acceptance
- Open access: articles freely available online
- High visibility within the field
- Retaining the copyright to your article

---

Submit your next manuscript at ► [springeropen.com](http://springeropen.com)